PNAS
Proceedings of the National Academy of Sciences of the United States of America www.pnas.org

Viral activation and recruitment of metacaspases in the unicellular coccolithophore, Emiliania huxleyi

Kay D. Bidle, Liti Haramaty, Joana Barcelos e Ramos, and Paul Falkowski

PNAS published online Mar 28, 2007;
doi:10.1073/pnas.0701240104

Viral activation and recruitment of metacaspases in the unicellular coccolithophore, *Emiliania huxleyi*

Kay D. Bidle*†, Liti Haramaty*, Joana Barcelos e Ramos*‡, and Paul Falkowski*§

*Environmental Biophysics and Molecular Ecology Group, Institute of Marine and Coastal Sciences, Rutgers, The State University of New Jersey, 71 Dudley Road, New Brunswick, NJ 08901; ‡Leibniz Institute for Marine Sciences (IFM-GEOMAR), 20 Düsternbrooker, 24105 Kiel, Germany; and §Department of Geological Sciences, Rutgers, The State University of New Jersey, Piscataway, NJ 08854

Communicated by James L. Van Etten, University of Nebraska, Lincoln, NE, February 17, 2007 (received for review November 21, 2006)

Lytic viral infection and programmed cell death (PCD) are thought to represent two distinct death mechanisms in phytoplankton, unicellular photoautotrophs that drift with ocean currents. Here, we demonstrate an interaction between autocatalytic PCD and lytic viral infection in the cosmopolitan coccolithophorid, *Emiliania huxleyi*. Successful infection of *E. huxleyi* strain 374 with a lytic virus, EhV1, resulted in rapid internal degradation of cellular components, a dramatic reduction in the photosynthetic efficiency (F_v/F_m), and an up-regulation of metacaspase protein expression, concomitant with induction of caspase-like activity. Caspase activation was confirmed through *in vitro* cleavage in cell extracts of the fluorogenic peptide substrate, IETD-AFC, and direct, *in vivo* staining of cells with the fluorescently labeled irreversible caspase inhibitor, FITC-VAD-FMK. Direct addition of z-VAD-FMK to infected cultures abolished cellular caspase activity and protein expression and severely impaired viral production. The absence of metacaspase protein expression in resistant *E. huxleyi* strain 373 during EhV1 infection further demonstrated the critical role of these proteases in facilitating viral lysis. Together with the presence of caspase cleavage recognition sequences within virally encoded proteins, we provide experimental evidence that coccolithoviruses induce and actively recruit host metacaspases as part of their replication strategy. These findings reveal a critical role for metacaspases in the turnover of phytoplankton biomass upon infection with viruses and point to coevolution of host–virus interactions in the activation and maintenance of these enzymes in planktonic, unicellular protists.

algal blooms | programmed cell death

Extremely high productivity to biomass ratios of marine phytoplankton imply that, on average, these planktonic, unicellular organisms turnover weekly (1). The molecular mechanisms regulating the lysis of phytoplankton cells have been virtually ignored, even though they serve to couple ≈50% of average global primary production to microbial foodwebs, effectively short circuiting carbon export to the deep ocean (2). The primary mechanism invoked by microbial ecologists to explain high lysis rates of phytoplankton populations (3–5) is exogenous infection by viruses (6, 7). Viruses are ubiquitous components of marine ecosystems, representing the most abundant entities in the ocean at 10^7 to 10^8 viruses per milliliter of surface seawater and exceeding bacterial and phytoplankton abundances by at least an order of magnitude (6, 7). Viral infection has been shown to influence large scale population dynamics of phytoplankton communities, through either bloom demise or "trimming" of host cell populations to non-bloom levels (6, 8, 9). Furthermore, viruses that are pathogenic to phytoplankton are routinely isolated from seawater by ultrafiltration (10), and the direct addition of these viruses to total seawater markedly reduces phytoplankton productivity and biomass (9).

Another possible mechanism to explain the high lysis rates in prokaryotic and eukaryotic unicellular phytoplankton, independent of viral attack, is autocatalytic cell death. This cellular self-destruction process is triggered by specific environmental stresses (e.g., cell age, nutrient deprivation, high light, oxidative stress, and UV exposure) (11–17) and is analogous to programmed cell death (PCD) in multicellular organisms. PCD involves the expression and biochemical coordination of specialized cellular machinery such as receptors, adaptors, signal kinases, proteases, and nuclear factors. A specific class of intracellular cysteinyl aspartate-specific proteases (i.e., caspases) is of particular interest because of their ubiquitous role in both initiation and execution of PCD through the cleavage of various essential proteins in response to proapoptotic signals (18).

The discovery of caspase orthologues, paracaspases and metacaspases, in morphologically diverse organisms including animals, higher plants, slime moulds, unicellular protists, fungi, and bacteria (19) suggests that they may represent an initial, ancestral core of executioners that led to the emergence of the cell death machinery. Presumably, early ancestors of plants and animals had minimal apoptotic machinery, with the more complex PCD systems emerging with the evolution of metazoans. Whereas most metacaspase genes have only been characterized *in silico*, their genetic signatures have been directly linked to caspase activity and the mediation of PCD in yeast (20) and trypanosomes (21). Metacaspases are also essential for PCD execution in plants despite possessing an altered substrate specificity compared with canonical caspases (22, 23). Nonetheless, the cellular roles of metacaspases still remain an open question in most unicellular protists, including phytoplankton.

Metacaspases (along with other putative PCD-related proteins) are widespread among prokaryotic and eukaryotic phytoplankton genomes (11). Moreover, morphological and biochemical characteristics that are consistent with caspase-mediated PCD have been observed in widely diverse evolutionary lineages of prokaryotic and eukaryotic phytoplankton, including cyanobacteria, chlorophytes, and dinoflagellates (12–15). The acquisition of PCD-related genes, like metacaspases, by unicellular phytoplankton and the processes that selected for their retention over an ≈3-billion-year evolutionary history remain unknown, leading to discussions about potential evolutionary drivers and ecological roles (11). Activation of PCD in unicellular organisms may have a viral connection, perhaps evolving as a defense mechanism to prevent massive viral infection (and demise) of clonal populations (24). Viral gene products are known to employ diverse regulatory roles in animal apoptosis (25) with a number of viruses actually inducing apoptosis and some specifically inducing caspases (26). Similarly, cytotoxic proteins ("killer toxins") encoded by double-stranded RNA viruses induce caspase-mediated apoptosis in yeast (27), and infection of plants by microbial pathogens triggers the hypersensitive response, a rapid form of

Author contributions: K.D.B. designed research; K.D.B., L.H., and J.B.e.R. performed research; K.D.B. contributed new reagents/analytic tools; K.D.B., L.H., J.B.e.R., and P.F. analyzed data; and K.D.B. and P.F. wrote the paper.

The authors declare no conflict of interest.

Freely available online through the PNAS open access option.

Abbreviations: PCD, programmed cell death; TEM, transmission electron microscopy; EhMC, *E. huxleyi* metacaspase; RuBisCo, ribulose-1,5-bisphosphate carboxylase-oxygenase.

†To whom correspondence should be addressed. E-mail: bidle@marine.rutgers.edu.

This article contains supporting information online at www.pnas.org/cgi/content/full/0701240104/DC1.

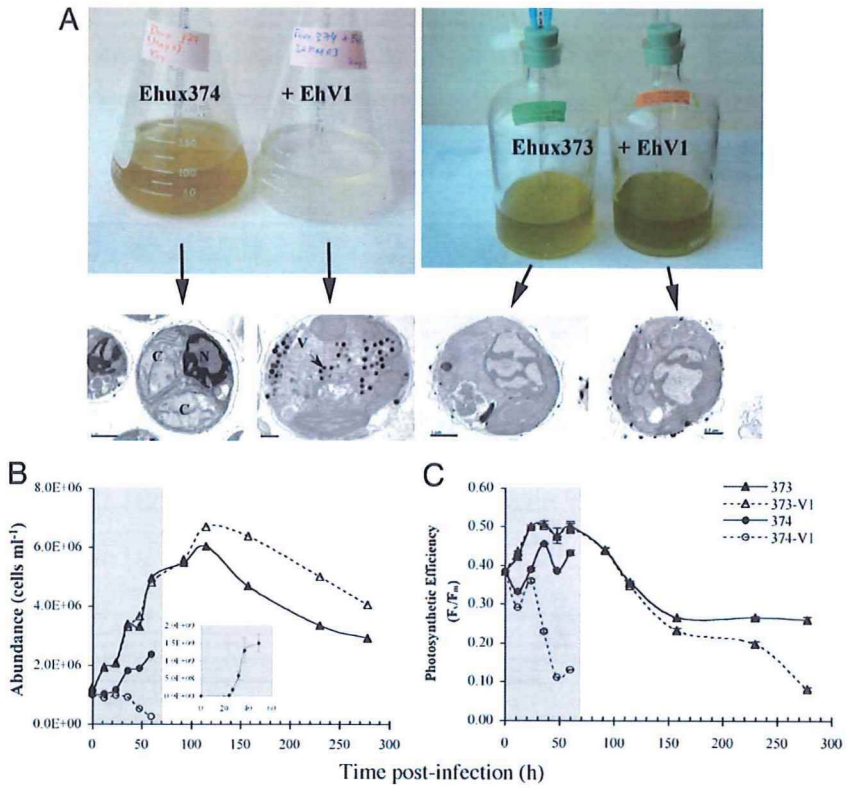

Fig. 1. EhV1 infection of "sensitive" *Ehux374* and "resistant" *Ehux373*. (*A*) Visual comparison of control and infected cultures 60 h after infection. Arrows and inset panels show TEM micrographs of cells collected 24 h after infection (C, chloroplast; N, nucleus; V, virus). (*B* and *C*) Time course of cell growth (*B*) and photosynthetic efficiency (*C*). *Ehux374* cultures were terminated after the 60-h viral time course (shading), whereas *Ehux373* cultures were allowed to grow into stationary and death phases. (*B Inset*) Time course of viral abundance during the 60-h infection period for *Ehux374*. No increase in viral abundance was detected for *Ehux373*.

PCD mediated by caspase-like proteases to restrict pathogen growth (28).

Emiliania huxleyi (Prymnesiophyte, Haptophyceae) belongs to the "coccolithophores," a class of unicellular phytoplankton with chromophyte lineage that dominates the modern ocean (29) and significantly contributes to the oceanic carbon cycle and biological pump through active precipitation of calcium carbonate. *E. huxleyi* is by far the most abundant and cosmopolitan coccolithophore on a global basis, forming massive annual blooms in the North Atlantic, which are routinely infected and terminated by double-stranded DNA-containing, lytic viruses (8, 30, 31). Numerous viruses specific to *E. huxleyi* have been isolated (8, 30) and, as a consequence, they are among the most studied eukaryotic phytoplankton host–virus systems to date. Nonetheless, specific cellular mechanisms triggered during execution of lytic viral infection are unknown. In this paper, we investigate the mechanistic interaction between viral infection of *E. huxleyi* and the host's metacaspase biochemical machinery.

Results and Discussion

Infection of *E. huxleyi* strain 374 (*Ehux374*) with the lytic virus, EhV1 (8), resulted in ≈90% reduction in cell abundance within 60 h because of cell lysis (Fig. 1 *A* and *B*). A dramatic increase in EhV1 production (Fig. 1*B Inset*) occurred concomitantly with the demise of *E. huxleyi* (Fig. 1*B Inset*). Viral abundance peaked in excess of 3×10^9 per ml, corresponding to a mature burst size of ≈800 viruses per cell. Transmission electron microscopy (TEM) analysis confirmed viral infection after 24 h, observed as visible electron-dense icosahedral particles replicating within the cytoplasm, along with internal degradation of organelles. Agarose gel electrophoresis revealed considerable DNA smearing after 48 h (data not shown). EhV1 infection significantly impaired the maximum photochemical quantum yield of photosystem II (F_v/F_m), declining by 51% and 72% after 36 h and 48 h, respectively (Fig. 1*C*). Healthy, uninfected control cells had compact, well-defined organelles, growth rates of up to 0.9 per day, and maintained $F_v/F_m > 0.4$ (Fig. 1 *A* and *C*). Cultures of *E. huxleyi* strain 373 (*Ehux373*), which normally displayed resistance to EhV1 infection (30) by means of a yet unknown mechanism, also showed no signs of clearing after 60 h (Fig. 1*A*). Cell abundance and F_v/F_m in the infected *Ehux373* culture mimicked that of the control over the first 60 h (Fig. 1 *B* and *C*, shaded area) and little to no DNA degradation was detected (data not shown).

EhV1infection of *Ehux374* triggered as much as an ≈200-fold increase in caspase specific activity in cell extracts, assessed *in vitro* through cleavage of the fluorogenic canonical caspase tetrapeptide substrate, Ile-Glu-Thr-Asp-7-amino-4-trifluoromethylcoumarin (IETD-AFC). Caspase specific activity generally peaked during the late phase (>30 h) of lytic cycle (Fig. 2*A*), whereas uninfected control cultures displayed <1% of this peak activity. In contrast, caspase activity in the resistant strain, *Ehux373*, infected with EhV1 remained low and was comparable with *Ehux374* control. However, *Ehux373* possessed caspase biochemical potential, as evidenced by steady increases (by a factor of 5–7) in caspase specific activity (Fig. 2*B*) for dying *Ehux373* batch cultures (>100 h). These cultures displayed simultaneous physiological stress and death, exhibiting mortality rates of 0.2–0.3 per day and a steady decrease in F_v/F_m to ≈0.2 (Fig. 1 *B* and *C*).

Caspase activation was confirmed by direct staining of *E. huxleyi* cells with a fluoroisothiocyanate (FITC) conjugate of the

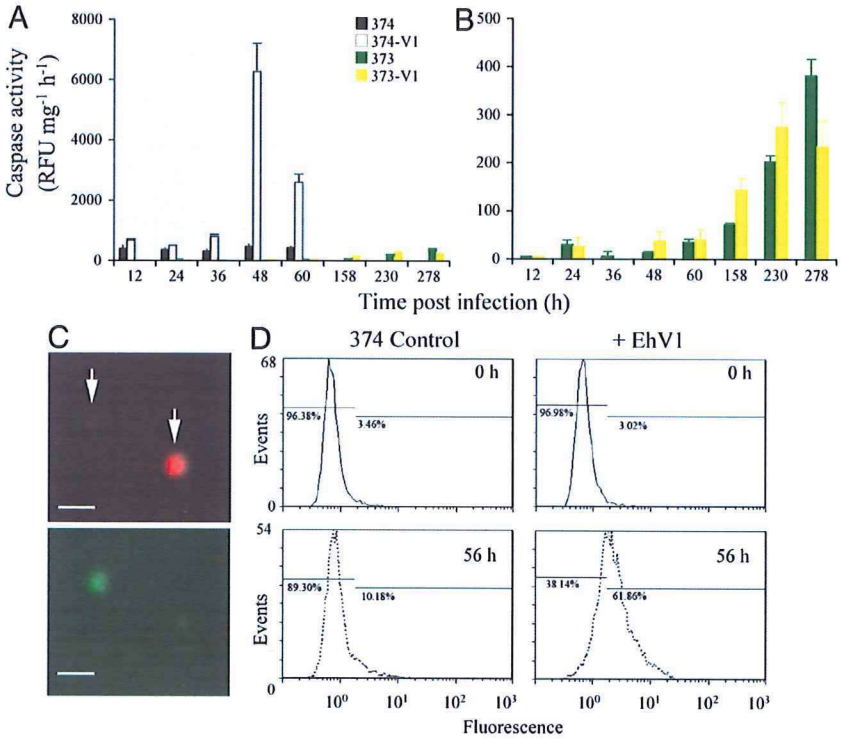

Fig. 2. Caspase activation in *E. huxleyi* by EhV1 infection. (*A*) Caspase-specific activity measured by the cleavage of IETD-AFC in *Ehux374* and *Ehux373* cell extracts. Error bars represent standard deviations among triplicate measurements. Shaded region represents the 60-h infection window. (*B*) Caspase activity for *Ehux373* cell extracts (in *A*) plotted on a different scale to illustrate activity increases in dying batch cultures ($t > 158$ h). (*C*) Epifluorescence micrographs showing fluorescence of *Ehux374* attributable to cellular chlorophyll (*Upper*) and staining with CaspACE FITC-VAD-FMK (*Lower*). Identical fields containing two cells are pictured (arrows). Note that the bright autofluorescent cell has minimal staining with CaspACE, whereas the dim autofluorescent (i.e., photosynthetically unhealthy) cell displays much brighter CaspACE staining. (Scale bars: 5 μm.) (*D*) Plots of the fluorescence distribution for CaspACE-stained control and EhV1-infected cell populations collected at 0 h and 56 h after infection and measured by flow cytometry (5,000 cells counted); inset lines designate the percentage of cells associated with each gate position.

broad-spectrum caspase inhibitor, z-Val-Ala-Asp-fluoromethylketone (z-VAD-FMK). VAD-FMK-FITC freely diffuses into cells and irreversibly binds to activated caspases, thus serving as an *in vivo* marker. Effective staining of *Ehux374* with VAD-FMK-FITC was observed for photosynthetically unhealthy cells, identified by their weak red autofluorescence (Fig. 2*C*). The percentage of positively stained *E. huxleyi* cells, quantified by flow cytometry, was dramatically elevated in virus-infected cultures (Fig. 2*D*). A very small percentage (<2.9%) of cells were positively stained at the time of infection, increasing at 36 h (30.3%), peaking at 56 h (61.2%), and subsequently dropping at 60 h (49.0%). Over this time, there was a clear shift in the virally infected *Ehux374* population toward increased fluorescence (≈5-fold) compared with the control culture at the same time points (Fig. 2*D*). Less than 10.2% of cells in the uninfected control culture were positively stained up through 56 h. Likewise, only 5.1–8.7% of resistant *Ehux373* cells were stained with VAD-FMK-FITC over this time period, corroborating the low IETD-AFC hydrolysis rates for this host strain. Both methods used to detect caspase activation in *Ehux374* revealed a strong dependence on mortality rate [supporting information (SI) Fig. 5; $r^2 > 0.75$].

Metacaspase transcripts have been detected in *E. huxleyi* by using expressed sequence tag (EST) libraries (32), with putative proteins resembling metacaspases from yeast and trypanosomes (11). To examine the expression and potential posttranslational modification of *E. huxleyi* metacaspases in response to viral infection, we overexpressed and purified a recombinant 36-kDa *E. huxleyi* metacaspase (EhMC) protein and generated polyclonal antibodies. Western blot analysis of cell extracts revealed constitutive expression of ≈36-kDa and ≈42-kDa metacaspase proteins in control *Ehux374* cells during a 60-h time course (Fig. 3*A Left*). EhV1 infection triggered a sharp increase in the intensity of the 42-kDa protein, concomitant with spikes in caspase specific activity (Fig. 2*A*). In stark contrast, no EhMC proteins were detected in *Ehux373* resistant cells during the 60-h viral infection time period (Fig. 3*A Right*). *Ehux373* did, however, show clear induction of an ≈50-kDa protein in dying batch cultures ($t = 278$ h), consistent with observations of elevated caspase activity (Fig. 2*B*).

Remarkably, the EhMC polyclonal antibody displayed strong, specific immunohybridization to purified, recombinant human caspase 8 (Fig. 3*B*), revealing fundamental epitope conservation between EhMC and canonical metazoan caspases despite their distant relatedness within the caspase superfamily (11). No hybridization was observed when caspase 8 was incubated with preimmune rabbit serum or with polyclonal antisera to ribulose-1,5-bisphosphate carboxylase-oxygenase (RuBisCo) (Fig. 3*B*), further confirming specificity of the EhMC antibody for caspase 8. These results demonstrate that lytic viral infection up-regulates EhMC expression and activity, concomitant with cell lysis, and suggest that metacaspases are responsible for the observed caspase activity in *E. huxleyi*. Plant metacaspases have slightly altered catalytic activity from metazoan caspases, despite conservation of the histidine-cysteine catalytic diad. Instead, they preferentially cleave at arginine/lysine (22, 23) rather than aspartate residues, perhaps mediating PCD through the activation of unknown, downstream cysteine proteases with caspase catalytic activity.

To test whether caspase activity was required for viral propagation, we applied z-VAD-FMK to EhV1 infected *Ehux374*

MICROBIOLOGY

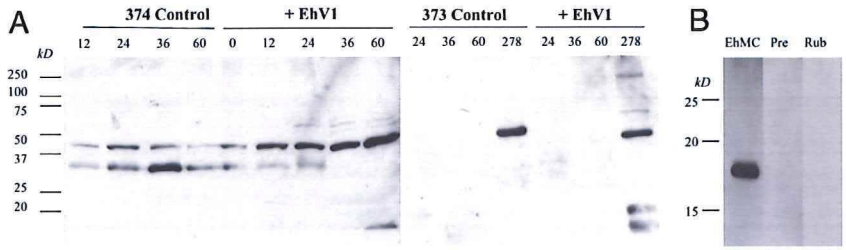

Fig. 3. Detection of metacaspase expression in *E. huxleyi*. (*A*) Western blot analysis of *Ehux374* (*Left*) and *Ehux373* (*Right*) cell extracts collected during a time course of viral infection, showing immunohybridization to polyclonal antibodies generated against a purified, recombinant *E. huxleyi* metacaspase protein (EhMC). Lane numbers represent collection time (hours after infection). Cell extracts correspond to samples presented in Figs. 1 and 2. (*B*) Western blot analysis testing immunohybridization of purified, recombinant human caspase 8 (10 ng per lane) to the following antisera: EhMC, polyclonal antisera generated against a purified, recombinant EhMC; Pre, preimmune serum collected before injection of EhMC; Rub, polyclonal antisera generated against purified RuBisCo. Banding is consistent with the expected ≈18-kDa subunit for caspase 8, according to the manufacturer. Molecular masses (in kilodaltons) are indicated.

cultures and assessed its effect on host physiology and viral production. The efficacy of z-VAD-FMK inhibition was dose-dependent. At a 20 μM concentration, the inhibitor effectively abolished cellular caspase activity by as much as 94% at 37 h after infection (Fig. 4*A*, triangles) and resulted in a marked reduction in EhMC expression (Fig. 4*A Inset*). Caspase inhibition delayed but did not abolish viral infection (Fig. 4*B*); cells had a 30–60% higher chance of survival when metacaspases were inhibited. In effect, the addition of 20 μM z-VAD-FMK selected for a subpopulation, resembling the resistant phenotype (*Ehux373*). Caspase inhibition also led to a doubling of photosynthetic efficiency (Fig. 4*C*) and severely impaired viral production (by 47–96%) and burst size (by 47–87%) (Fig. 4*D*).

When EhMC expression was undetectable in the resistant strain (*Ehux373*) or dramatically reduced in the z-VAD-FMK-treated sensitive strain (*Ehux374*), viral lysis was greatly attenuated, if not eliminated. In contrast, when *Ehux373* constitutively expressed EhMC proteins, it displayed transient susceptibility to EhV1 (SI Figs. 6 and 7). In *Ehux373* cells infected by EhV1, metacaspase expression was characterized by an additional ≈50 kDa protein (>34 h) and the associated caspase specific activity was comparable with infected *Ehux374* (SI Fig. 6 *A* and *B*). Concurrently, growth was dramatically reduced (0.01–0.07 per day) up to 58 h (SI Fig. 7*A*). TEM images revealed successful infection of *Ehux373* between 24–36 h, with some cells containing replicating viruses (SI Fig. 7*B*). Rather than completely lyse, *Ehux373* subsequently recovered and grew. No replicating viruses were observed in cells during recovery. Infected *Ehux373* also had both higher photosynthetic efficiency and lower viral production compared with infected *Ehux374* (SI Fig. 7 *C* and *D*), and displayed notable differences in metacaspase expression >58 h after infection (SI Fig. 6), during recovery. Given the original single-cell isolation of *Ehux373* from the North Atlantic, our observations suggest that differential metacaspase expression and activation within a clonal population of cells may influence viral susceptibility.

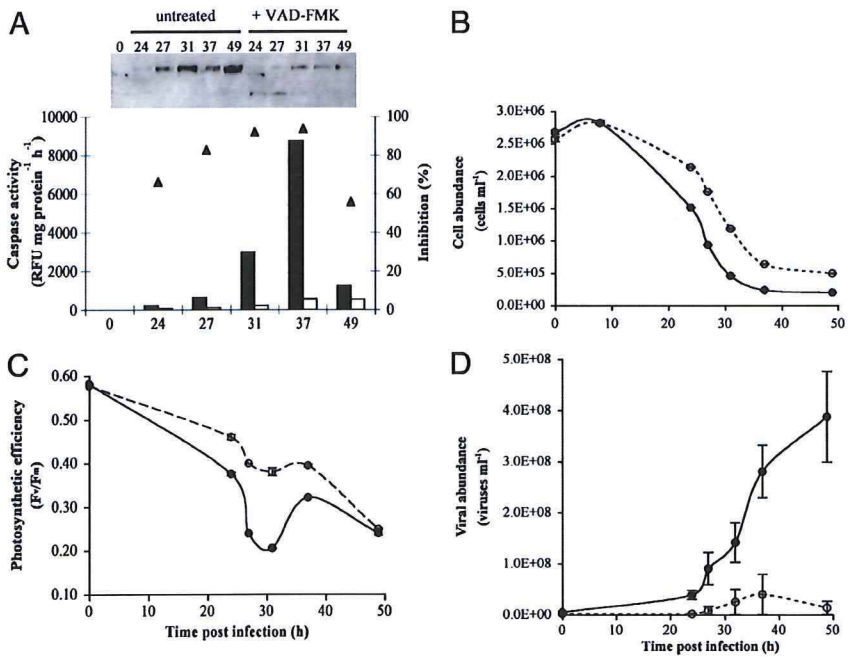

Fig. 4. The effect of *in vivo* addition of 20 μM z-VAD-FMK on EhV1 infection of *Ehux374*. (*A*) Caspase specific activity from cells incubating with (open bars) and without (filled bars) z-VAD-FMK, including the degree of inhibition (%; triangles). (*Inset*) Western blot analysis of these same cell extracts showing reduced hybridization to EhMC antisera in inhibited samples. (*B–D*) Effect of inhibitor treatment (open circles, dashed line) relative to DMSO-only additions (filled circle, solid line) on *E. huxleyi* cell abundance (*B*), photosynthetic efficiency (*C*), and viral production (*D*), expressed as viral abundance in the media. Error bars represent the standard deviation for triplicate measurements.

Table 1. *Phycodnaviridae* proteins with caspase cleavage sites

Gene ID (accession no.)	Putative function	Cleavage sequence
E. huxleyi virus strain 86		
EhV146 (YP_293899)	Putative membrane protein	LEHD
EhV153 (CA165575)	Hypothetical protein	VEID
EhV158 (YP_293911)*	Putative DNA ligase	YVAD
EhV218 (YP_293973)	Hypothetical protein	DEVD
EhV325 (YP_294083)	Putative membrane protein	YVAD
EhV348 (YP_294106)	Alkylated DNA repair protein	LEHD
EhV368 (YP_294126)	Hypothetical protein	DEVD
EhV403 (YP_294161)*	Hypothetical protein	DEVD†
E. siliculosus virus		
EhV-1-14 (NP_077499)	Histidine kinase	IETD
EsV-1-75 (NP_077560)*	Cathepsin B	YVAD
EsV-1-93 (NP_077578)	DNA polymerase, type B	VEID
EsV-1-231 (NP_077716)	Unknown	YVAD
P. bursaria Chlorella virus 1 (NP_048749)	ATPase	YVAD

*Conserved core NCLDV genes (39).
†Two cleavage sites present.

The severe reduction of viral replication by selective caspase inhibition suggests that the replication process requires activation of host metacaspases. Similar observations have been made for several animal viruses (26), where caspase activity is required for replication and point mutation of caspase cleavage sequences on viral proteins abolishes viral replication (26). Inspection of the genome sequence of *E. huxleyi* lytic virus strain 86 (EhV86) (33), the type species of the *Coccolithovirus*, uncovered several viral proteins possessing signature caspase tetrapeptide cleavage sequences (Table 1). Microarray analysis has profiled expression of these viral proteins to primary (1 h) and secondary (2–4 h) transcriptional phases during infection (34). Moreover, the EhV86 genome contains biosynthetic genes for ceramide (33), a known inducer of PCD via a sphingolipid pathway (35), one of which, serine palmitoyltransferase, was recently overexpressed in yeast and shown to be fully functional (36). Importantly, infection of *Ehux374* with EhV86 triggered caspase activation in a manner similar to EhV1 (data not shown). Taken together, our findings support the late-phase (>30 h) induction and active recruitment of the host's PCD execution machinery by coccolithoviruses. It is tempting to speculate that this recruitment may represent a conserved strategy among the broad, monophyletic *Phycodnaviridae* family of giant icosahedral dsDNA viruses infecting eukaryotic phytoplankton (37, 38), which encompass the *Coccolithovirus*. Indeed, virally encoded proteins containing caspase cleavage sequences were also found in the only other *Phycodnaviridae* genome sequences completed to date, *Ectocarpus siliculosus* virus (EsV-1) and *Paramecium bursaria Chlorella* virus 1 (PBCV-1) (Table 1). Remarkably, a few of these caspase cleavage-containing proteins represent a group of "core" genes, shared among several families of nucleocytoplasmic large DNA viruses (NCDLV) and thought to represent an ancestral viral genome (39), thus arguing for early development within this viral lineage.

Recruitment of *E. huxleyi* metacaspases by coccolithoviruses, as part of their replication program, points to the coevolution of virus-host interactions in the activation and maintenance of the PCD machinery. The "Red Queen" hypothesis governing the evolution of host-parasite relationships (40) argues for an intense "arms race" between viral strains, trying to maximize virulence, and host strains, trying to minimize virulence, resulting in an intense selection pressure that stimulates genetic diversity. Our findings raise fundamental questions about the nature of these virus-host interactions, such as the physiological state and genetic diversity of *E. huxleyi* and its influence on viral resistance. Whereas strains of *E. huxleyi*-specific viruses display a high host-specificity (30), resistance may not be a fixed trait, perhaps undone by metacaspase expression under physiological stress. Indeed, highly specific, coevolutionary processes in the activation and maintenance of metacaspases may contribute to the diversification and specificity of coccolithophores (41) and their viruses and influence which strains escape viral trimming to form blooms.

Methods

Culture Maintenance and Growth Conditions. *E. huxleyi* (strains CCMP 373 and 374) was obtained from the Provasoli-Guillard Center for Culture of Marine Phytoplankton (CCMP) and batch grown in f/2 medium (minus Si) at 18°C, 14:10 (L:D) cycle and ≈450 μmol quanta $m^{-2}{\cdot}s^{-1}$ with constant aeration. Cell abundance was determined by using a Coulter Multisizer II (Beckman Coulter, Fullerton, CA). Fast repetition rate fluorometry was used to derive the maximum photochemical quantum yield of photosystem II (F_v/F_m), an indicator of photosynthetic health.

Viral Infection. EhV1 and EhV86 were obtained courtesy of G. Bratbak (University of Bergen, Bergen, Norway) and W. Wilson (Bigelow Laboratory for Ocean Sciences, West Boothbay Harbor, ME), respectively. Both viral strains were propagated by using batch cultures of *E. huxleyi* 374 grown in f/2 (minus Si). In each case, a master *Ehux374* culture was grown to a cell density of ≈1×10^6 cells per ml and, subsequently, split into two equal components, one representing a virus-free control and one infected with EhV1, at a multiplicity of infection of ≈5. Viral lysates were centrifuged (10,000 × *g*, 4°C, 10 min) and passed through 0.4-μm polycarbonate filters to remove cellular and particulate debris before infection. EhV1 viral particles were directly visualized and enumerated by using epifluorescence microscopy (Zeiss Axioskop), after staining with 10× SYBR Gold (Molecular Probes, Eugene, Oregon) in PBS and filtration onto 0.02-μm pore-size Anodisc filters.

TEM. Cells were pelleted by means of centrifugation (10,000 × *g*, 4°C, 10 min), washed with 0.2-μm filtered seawater, and preserved in Trump's EM fixative (4% formaldehyde/1% glutaraldehyde in phosphate buffer, pH 7.2) for at least 4 h at 4°C. Fixed cells were rinsed three times (2 × 15 min) in Milloning's phosphate buffer, pH 7.3, postfixed for 2 h in 1% buffered OsO_4, washed three times, and dehydrated through a graded series of ethanol. After replacement of ethanol with propylene oxide, cells were embedded in Epon-Araldite mixture. Sections were cut by using a LKB 2088 ultramicrotome, collected on 200-mesh copper grids, and stained with uranyl acetate and lead citrate. The stained sections were photographed in a JEM-100CXII electron microscope.

Detection and Measurement of Caspase Activity. *E. huxleyi* cells were pelleted by means of centrifugation (10,000 × *g*, 4°C, 10 min), frozen in liquid nitrogen, and stored at −80°C until processed. Cells were resuspended in caspase activity buffer [50 mM Hepes (pH 7.3)/100 mM NaCl/10% sucrose/0.1% CHAPS/10 mM DTT] and sonicated, and cellular debris was pelleted by means of centrifugation (16,000 × *g*; room temperature; 2 min). Cell extracts were incubated with 50 μM IETD-AFC (Calbiochem, San Diego, CA) for 4 h at 25°C. Fluorescence was measured by using a Spectra Max Gemini XS plate reader (excitation 400 nm, emission 505 nm). Activity was abolished (>95%) with the irreversible caspase inhibitor z-VAD-FMK (Calbiochem).

Intact *E. huxleyi* cells were also directly stained *in situ* with CaspACE FITC-VAD-FMK (Promega, Madison WI). Cells were pelleted by means of centrifugation, washed once with PBS (pH 7.5), and resuspended in PBS before the addition of CaspACE (final concentration, 20 μM). Cells were stained for 20 min at 18°C

in the dark, after which they were pelleted by means of centrifugation, washed once with PBS, fixed with 2% formalin/PBS, and stored at 4°C until analyzed (within 1 week). An unstained control was performed for each time point. Cells were directly visualized and photographed by using epifluorescence microscopy. The percentage of cells stained with CaspACE was determined by flow cytometry (5,000 cells counted).

z-VAD-FMK was added directly to cultures at a final concentration of 20 μM to both healthy control cultures and those infected with EhV1. Inhibitor spikes were performed at the time of viral infection. Because z-VAD-FMK was dissolved in dimethyl sulfoxide (DMSO), DMSO-only spikes (0.1% final concentration) were run in parallel as controls.

Flow Cytometry Analysis. Samples were run on a Beckman Coulter Cytomics FC500 Flow Cytometer (Flow Cytometry Core Facility, Environmental and Occupational Health and Safety Institute, Rutgers University) using a designated FITC protocol. An unstained control was used for each sample set (sampling time and culture type) to gate *E. huxleyi* cells based on side-scatter (size), forward scatter (granularity), and fluorescence. Five thousand cells were counted for each sample.

Generation of EhMC Antibody. A full-length *E. huxleyi* metacaspase transcript (32) was cloned and overexpressed in *Escherichia coli* (Rosetta 2-DE3-pLysS host) by using pET14b expression vector (Novagen, San Diego, CA), according to the manufacturer's protocols. The overexpressed fusion protein, which was localized to insoluble inclusion bodies in *E. coli*, was extracted in 7 M Urea and purified via the N-terminal His-Tag sequence by using a SuperFlo Ni-NTA column and HPLC. The EhMC was further gel-purified on SDS/PAGE prep gels. Purity was verified by silver staining and by Western blot analysis with a monoclonal 6X-His antibody. Two milligrams of EhMC recombinant protein was injected per New Zealand White rabbit as an initial boost (Laboratory Animal Services, Rutgers University). Subsequent injection boosts of 1 mg of protein per rabbit were performed monthly. Serum was removed from each rabbit monthly. Serum titer and specificity to EhMC were verified by using purified EhMC protein, *E. huxleyi* cell extracts, and IPTG-induced pET14b-containing and pET14b-absent *E. coli* extracts. Preimmune serum was collected before the injection of purified EhMC protein.

Western Blot Analysis. *E. huxleyi* cell extracts were loaded with equal amounts of protein, separated on 10% SDS/PAGE gels, and transferred onto PVDF membranes. Membranes were probed with polyclonal antisera against recombinant EhMC (1:500) and polyclonal goat anti-rabbit IgG (Pierce; 1:30,000), followed by horseradish peroxidase chemiluminescence detection (SuperSignal; Pierce, Rockford, IL). Purified recombinant caspase 8, derived from human cDNA encoding residues identical to Ser-217 to Asp-479 (C terminus; Swiss-Prot accession no. Q14790), was purchased commercially (BioMol, Plymouth Meeting, PA). Ten nanograms of caspase 8 were loaded into replicate lanes and subjected to 15% SDS/PAGE, transferred to PVDF membranes, and probed with EhMC antisera, preimmune antisera (collected from same rabbits before injection with purified EhMC; 1:500), or polyclonal antisera to RuBisCo (1:500).

Viral Genome and Protein Sequences. Predicted protein sequences from the complete genomes of *Phycodnaviridae* were obtained from the Genomes Division of the Entrez system (National Center for Biotechnology Information, National Institutes of Health, Bethesda, MD; www.ncbi.nlm.nih.gov/entrez/query.fcgi?DB=Genome) and the Giant Virus Genome web site (www.giantvirus.org/).

We thank Cyndi Corwonski and Sara Bender for laboratory assistance, Valentin Starovoytov for TEM analysis, Sang Hoon Lee for help with expression and purification of recombinant metacaspase, Kate McGuirk for help with antibody generation, Petra Flam for flow cytometry assistance, Julie Sexton and Bob Guillard at the Provasoli-Guillard Center for Culture of Marine Phytoplankton for help regarding the isolation history of *Ehux373*, Assaf Vardi for stimulating discussions, and Herman Spaink (Leiden University, Leiden, The Netherlands) for generously providing the EhMC clone. This work was supported by National Science Foundation Grant IOB-0414536 (to K.D.B. and P.F.).

1. Field CB, Behrenfeld MJ, Randerson JT, Falkowski P (1998) *Science* 237–240.
2. Azam F (1998) *Science* 280:694–696.
3. Agustí S, Satta MP, Mura MP, Benavent E (1998) *Limnol Oceanogr* 43:1836–1849.
4. Brussaard CPD, Riegman R, Noordeloos AAM, Cadée GC, Witte H, Kop AJ, Nieuwland G, Duyl FCV, Bak RPM (1995) *Mar Ecol Prog Ser* 123:259–271.
5. vanBoekel WHM, Hansen FC, Riegman R, Bak RPM (1992) *Mar Ecol Prog Ser* 81:269–276.
6. Suttle CA (1994) *Microb Ecol* 28:237–243.
7. Fuhrman JA (1999) *Nature* 399:541–548.
8. Bratbak G, Egge JK, Heldal M (1993) *Mar Ecol Prog Ser* 93:39–48.
9. Suttle CA, Chan AM, Cottrell MT (1990) *Nature* 347:467–469.
10. Suttle CA, Chan AM, Cottrell MT (1991) *Appl Environ Microbiol* 57:721–726.
11. Bidle KD, Falkowski PG (2004) *Nat Rev Microbiol* 2:643–655.
12. Berman-Frank I, Bidle K, Haramaty L, Falkowski P (2004) *Limnol Oceanogr* 49:997–1005.
13. Vardi A, Berman-Frank I, Rozenberg T, Hadas O, Kaplan A, Levine A (1999) *Curr Biol* 9:1061–1064.
14. Moharikar S, D'Souza JS, Kulkarni AB, Rao BJ (2006) *J Phycol* 42:42–433.
15. Segovia M, Haramaty L, Berges JA, Falkowski PG (2003) *Plant Physiol* 132:99–105.
16. Brussaard CPD, Noordeloos AAM, Riegman R (1997) *J Phycol* 33:980–987.
17. Berges JA, Falkowski PG (1998) *Limnol Oceanogr* 43:129–135.
18. Thornberry NA, Lazebnik Y (1998) *Science* 281:1312–1316.
19. Uren AG, O'Rourke K, Pisabarro MT, Seshagiri S, Koonin EV, Dixit VM (2000) *Mol Cell* 6:961–967.
20. Madeo F, Herker E, Maldener C, Wissing S, Lächelt S, Herlan M, Fehr M, Lauber K, Sigrist SJ, Wesselborg S, Fröhlich K-U (2002) *Mol Cell* 9:911–917.
21. Szallies A, Kubata BK, Duszenko M (2002) *FEBS Lett* 517:144–150.
22. Bozhkov PV, Suarez MF, Filonova LH, Daniel G Jr., AAZ, Rodriguez-Nieto S, Zhivotovsky B, Smertenko A (2005) *Proc Natl Acad Sci USA* 102:14463–14468.
23. Watanabe N, Lam E (2005) *J Biol Chem* 280:14691–14699.
24. Georgiou T, Yu Y-TN, Ekunwe S, Buttner MJ, Zuurmond A-M, Kraal B, Kleanthous C, Snyder L (1998) *Proc Natl Acad Sci USA* 95:2891–2895.
25. Teodoro JG, Branton PE (1997) *J Virol* 71:1739–1746.
26. Best SM, Bloom ME (2004) *Virology* 320:191–194.
27. Reiter J, Herker E, Madeo F, Schmitt MJ (2005) *J Cell Biol* 168:353–358.
28. Lam E, Kato N, Lawton M (2001) *Nature* 411:848–853.
29. Falkowski PG, Katz ME, Knoll AH, Quigg A, Raven JA, Schofield O, Taylor FJR (2004) *Science* 305:354–360.
30. Schroeder DC, Oke J, Malin G, Wilson WH (2002) *Arch Virol* 147:1685–1698.
31. Jacquet S, Heldal M, Iglesias-Rodriguez D, Larsen A, Wilson W, Bratbak G (2002) *Aquat Microb Ecol* 27:111–124.
32. Wahlund TM, Hadaegh AR, Clark R, Nguyen B, Fanelli M, Read BA (2004) *Mar Biotechnol* 6:278–290.
33. Wilson WH, Schroeder DC, Allen MJ, Holden MTG, Parkhill J, Barrell BG, Churcher C, Hamlin N, Mungall K, Norbertczak H, *et al.* (2005) *Science* 309:1090–1092.
34. Allen MJ, Forster T, Schroeder DC, Hall M, Roy D, Ghazal P, Wilson WH (2006) *J Virol* 80:7699–7705.
35. Jarvis WD, Kolesnick RN, Fornari FA, Traylor RS, Gewirtz DA (1994) *Proc Natl Acad Sci USA* 91:73–77.
36. Han G, Gable K, Yan L, Allen MJ, Wilson WH, Moitra P, Harmon JM, Dunn TM (2006) *J Biol Chem* 281:39935–39942.
37. VanEtten JL, Graves MV, Müller DG, Boland W, Delaroque N (2002) *Arch Virol* 147:1479–1516.
38. Dunigan DD, Fitzgerald LA, VanEtten JL (2006) *Virus Res* 117:119–132.
39. Iyer LM, Aravind L, Koonin EV (2001) *J Virol* 75:11720–11734.
40. VanValen L (1973) *Evol Theory* 1:1–30.
41. deVargas C, Probert I, Aubry M-P, Young J (2007) in *Evolution of Primary Producers in the Sea*, eds Falkowski PG, Knoll AH (Academic, New York), Vol 1, in press.